

Review of Three Equivalent Approaches for Computing Electromagnetic Fields from an Extending Lightning Discharge

Rajeev Thottappillil^A and Vladimir A. Rakov^B

A. Division for Electricity and Lightning Research, Uppsala University, Box 534, 75121, Uppsala, SWEDEN.

B. Department of Electrical and Computer Engineering, University of Florida, Gainesville, Florida 32611-6130, USA

Abstract

Three different general approaches for calculating the electromagnetic fields at any point in space from a lightning return stroke, which is modelled as an extending linear antenna, are reviewed and compared. In the first approach, known as the dipole approach, the electric field is completely expressed in terms of the retarded current on the lightning channel and in the second approach the electric field is expressed in terms of the current and local charge density in retarded time. In the third approach the electric field is completely expressed in terms of the apparent charge density, that is, the charge density that would be seen in the channel by a remote observer at retarded time. In general, apparent charge density is different from the local charge density in retarded time. Analytically these three electric field expressions are equivalent, which is verified numerically also. Besides, it is shown that the magnetic field can be completely expressed in terms of the apparent charge density, as opposed to the traditional expression for magnetic field involving only the retarded current. It is also shown that the division of electric field into static, induction, and radiation field components are not unique in the first two approaches, even though the total field is the same. Numerical calculations of electric fields and magnetic fields predicted by the transmission line (TL) model of the return stroke are presented at different distances from origin and at different angles to the vertical for different return stroke speeds. This also provides a numerical verification of the general electric and magnetic field expressions from the third approach against the first approach.

Index Terms

Lightning, Return Stroke, Dipole, Monopole, Apparent Charge, Continuity Equation, Lorentz Condition, Electric and Magnetic Fields.

1 INTRODUCTION

Lightning discharge occurs in a thin (compared to overall length) channel. Usually we are interested in the electromagnetic fields created by lightning several tens of meters to kilometers away. Therefore, in calculating electric and magnetic fields from lightning, its channel is modelled as a linear antenna which has some current distribution or which has certain line charge density distribution that changes with time. Besides, lightning is a self-propagating discharge whose length extends at great speeds, sometimes a significant fraction of the speed of light. Therefore, field calculation requires careful consideration of the retardation phenomenon due to finite travel time of the signals at speed of light. In this paper, three different, but equivalent, analytical expressions for calculating the electric and magnetic fields from lightning are

reviewed. These are exact general expressions applicable to any line source distribution that varies with time.

1.1 Three approaches for calculating the electromagnetic fields

Expressions for electric and magnetic fields from an electric dipole in the frequency domain can be found in most books on electromagnetics. However, time domain expressions are the most suitable for lightning discharge since it is a transient event whose current and charge distributions change in space and time in a non-periodic manner. Besides, the lightning discharge propagates and hence the linear dimensions of the discharge increase with time, often at speeds of one-third to one-half the speed of light.

The problem of calculating the electric and magnetic fields from a known source distribution is discussed extensively in literature. Usually the fields are calculated by using scalar and vector potentials. These potentials are directly related to the source distribution.

There are three equivalent approaches to calculating the electric fields produced by a specified source. Two of these equivalent approaches are discussed in Rubinstein *et al.* [1], Safaeinili and Mina [2], and Thottappillil and Rakov [3,4], and the third equivalent approach in Thottappillil *et al.* [5] and [3]. The first approach, the so-called dipole technique or Lorentz condition technique, involves (e.g., Uman *et al.* [6]) the specification of current density \vec{J} , the use of \vec{J} to find the vector potential \vec{A} , the use of \vec{A} and the Lorentz condition to find the scalar potential ϕ , the computation of electric field \vec{E} using \vec{A} and ϕ , and the computation of magnetic field \vec{B} using \vec{A} .

In this technique, the source is described only in terms of current density, and both the electric and magnetic field equations are expressed only in terms of current. The use of the Lorentz condition eliminates the need for the specification of the line charge density along with the current density and assures that the current continuity equation, which is not explicitly used in this technique, is satisfied.

The second approach, the so-called monopole technique or the continuity equation technique, involves (e.g., Jefimenko [7]; Thomson [8]) the specification of current density \vec{J} , the use of \vec{J} and the continuity equation to find ρ , the use of \vec{J} to find \vec{A} , the use of ρ to find ϕ , the computation of electric field \vec{E} using \vec{A} and ϕ , and the computation of magnetic field \vec{B} using \vec{A} .

In this technique, the source is described in terms of both current density and charge density, and the electric field equations are expressed in terms of both charge density and current, whereas the magnetic field equation is completely expressed in terms of current. The current continuity equation is needed to relate the current density and charge density. There is no need for the explicit use of the Lorentz condition in this technique, although properly specified scalar and vector potentials do satisfy the Lorentz condition.

In the third approach, both the electric fields and magnetic fields are expressed in terms of the apparent charge density, that is, the charge density that would be 'seen' on the lightning channel by an observer at the

field point. The difference between this apparent charge density and the charge density in the second approach outlined above is discussed in [3] and is explained in Appendix A. Field equations obtained in either of the first two approaches can be converted into this third form.

A spherical coordinate system $(\hat{r}, \hat{\theta}, \hat{\phi})$ is adopted in presenting all the three approaches in the following sections.

2. FIELDS IN TERMS OF CURRENT (THE LORENTZ CONDITION APPROACH)

The lightning return-stroke channel can be modelled as a straight line fixed at one end A, with the other end extending with speed v . The geometry of the problem is shown in Fig. 1. The current on the lightning channel is represented by $i(z', t)$, where z' indicates the position along the z -axis with origin at the base of the channel and t indicates the time. At time $t=0$ the return stroke starts to propagate from origin A. The observer at the fixed field point P 'sees' the return stroke starting to propagate from the origin at time $t=r/c$, where c is the speed of light. The retarded current at any elemental channel section dz' is given by $i(z', t-R(z')/c)$, where z' is less than or equal to $L'(t)$, the length of the return stroke channel 'seen' by the observer at P at time t . Note that the assumption of constant return-stroke speed is not required for developing the concepts presented here.

In fact, the lightning channel can be considered to be composed of many electric dipoles of length dz' . An electric dipole is a linear current element whose length is vanishingly small compared to the distance at which the fields are to be calculated. Also, the current is assumed to be a constant over the length of the dipole. Field expressions in the time domain, with specific application to lightning, are introduced by [6], and further developed by [1], Rubinstein *et al.* [9], [5], Thottappillil *et al.* [10], [8] and [3, 4].

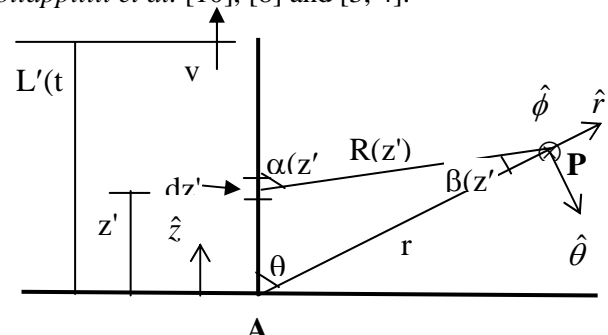


Figure 1: Geometry of the problem.

It takes a time r/c for the information from the channel-base A to reach the observer at P and hence the observer “sees” the channel emerging from A at time r/c . The actual length $L(t)$ of the channel at a time t is given by $L(t) = v \cdot t$. The apparent length of the channel at time t ‘seen’ by the observer at P is different from $L(t)$. This length can also be called the retarded length. If we define the time t such that it is the sum of the time required for the return-stroke wavefront to reach a height $L'(t)$ and the time required for a signal to travel from the wavefront at $L'(t)$ to the observer at P, t can be written as

$$t = \frac{L'(t)}{v} + \frac{R(L')}{c} \tag{1a}$$

where $R(L') = \sqrt{r^2 + L'^2(t) - 2L'(t)r \cos \theta}$ (1b)

The retarded length $L'(t)$ can be obtained by solving (1) and is given by [10]

$$L'(t) = \frac{r}{1 - \frac{v^2}{c^2}} \left[-\frac{v^2}{c^2} \cos \theta + \frac{vt}{r} - \frac{v}{c} \sqrt{\left(1 - \frac{v^2}{c^2}\right) + \frac{v^2 t^2}{r^2} + \frac{v^2}{c^2} \cos^2 \theta - \frac{2vt}{r} \cos \theta} \right] \tag{2}$$

The vector potential at P due to the entire extending channel at a time τ is given by

$$\bar{A}(r, \theta, \tau) = \frac{1}{4\pi\epsilon_0 c^2} \int_0^{L(\tau)} \frac{i(z', \tau - R(z'/c))}{R(z')} \hat{z} dz' \tag{3}$$

where τ is a time less than or equal to time t . At time τ , return-stroke wavefront is “seen” at a height $L'(\tau)$ by the observer at P and $L'(\tau)$ is less than or equal to $L'(t)$. Note that in equation (3) we have not considered the presence of ground, usually assumed to be perfectly conducting and replaced by the channel image.

2.1 Electric Field

The total electric field can be calculated using the relation

$$\bar{E} = -\nabla\phi - \frac{\partial\bar{A}}{\partial t} \tag{4}$$

where ϕ can be obtained from the Lorentz condition

$$\nabla \cdot \bar{A} + \frac{1}{c^2} \frac{\partial\phi}{\partial t} = 0, \text{ as}$$

$$\phi(r, \theta, t) = -c^2 \int_{r/c}^t \nabla \cdot \bar{A} d\tau \tag{5}$$

Taking the divergence of (3) it can be shown that

$$\nabla \cdot \bar{A}(r, \theta, \tau) = \frac{1}{4\pi\epsilon_0 c^2} \int_0^{L(\tau)} \left[\frac{z'-r \cos \theta}{R^3(z')} i(z', \tau - \frac{R(z')}{c}) + \frac{z'-r \cos \theta}{cR^2(z')} \frac{\partial i(z', \tau - R(z')/c)}{\partial \tau} \right] dz' + \frac{1}{4\pi\epsilon_0 c^2} \frac{L'(\tau) - r \cos \theta}{cR^2(L')} i(L', \tau - \frac{R(L')}{c}) \frac{dL'(\tau)}{d\tau} \tag{6}$$

Substituting (6) into (5) and interchanging the order of integration, an expression for the scalar potential completely in terms of current can be obtained. As time increases from r/c to t , the channel length $L'(\tau)$ increases monotonically from 0 to $L'(t)$. Therefore the order of integration can be changed as follows according to the standard rule.

$$\int_{r/c}^t \int_0^{L(\tau)} \Rightarrow \int_0^{L(t)} \int_{\tau}^t \tag{7}$$

where the lower limit $\tau = t_b$ is the time at which the observer at the field point ‘sees’ the return-stroke front at height z' for the first time. For a constant return-stroke speed v ,

$$\tau = \frac{L'(\tau)}{v} + \frac{R(L'(\tau))}{c} = \frac{z'}{v} + \frac{R(z')}{c}$$

Performing the operations explained above and after some reductions, we get an expression for scalar potential as [3]

$$\phi(r, \theta, t) = -\frac{1}{4\pi\epsilon_0} \int_0^{L(t)} \left[\frac{z'-r \cos \theta}{R^3(z')} \int_{\frac{z'+R(z')}{v}}^t i(z', t - \frac{R(z')}{c}) d\tau + \frac{z'-r \cos \theta}{cR^2(z')} i(z', t - \frac{R(z')}{c}) \right] dz' \tag{8}$$

Taking the gradient of equation (8), $\nabla\phi$, and the time derivative of equation (3), $\frac{\partial\bar{A}}{\partial t}$, we get an expression for electric field according to equation (4) as given below in equation (9):

$$\begin{aligned} \bar{E}(r, \theta, t) = & \\ & -\frac{1}{4\pi\epsilon_0} \hat{r} \int_0^{L(t)} \left[\frac{\cos \theta - 3 \cos \alpha(z') \cos \beta(z')}{R^3(z')} \right. \\ & \left. \cdot \int_{t_b}^t i(z', \tau - \frac{R(z')}{c}) d\tau \right] dz' \quad (a) \\ & -\frac{1}{4\pi\epsilon_0} \hat{r} \int_0^{L(t)} \left[\frac{\cos \theta - 3 \cos \alpha(z') \cos \beta(z')}{cR^2(z')} \right. \\ & \left. \cdot i(z', t - \frac{R(z')}{c}) \right] dz' \quad (b) \\ & -\frac{1}{4\pi\epsilon_0} \hat{r} \int_0^{L(t)} \left[\frac{\cos \theta - \cos \alpha(z') \cos \beta(z')}{c^2 R(z')} \right. \\ & \left. \cdot \frac{\partial i(z', t - R(z')/c)}{\partial t} \right] dz' \quad (c) \\ & +\frac{1}{4\pi\epsilon_0} \hat{\theta} \int_0^{L(t)} \left[\frac{\sin \theta + 3 \cos \alpha(z') \sin \beta(z')}{R^3(z')} \right. \\ & \left. \cdot \int_{t_b}^t i(z', \tau - \frac{R(z')}{c}) d\tau \right] dz' \quad (d) \\ & +\frac{1}{4\pi\epsilon_0} \hat{\theta} \int_0^{L(t)} \left[\frac{\sin \theta + 3 \cos \alpha(z') \sin \beta(z')}{cR^2(z')} \right. \\ & \left. \cdot i(z', t - \frac{R(z')}{c}) \right] dz' \quad (e) \\ & +\frac{1}{4\pi\epsilon_0} \hat{\theta} \int_0^{L(t)} \left[\frac{\sin \theta + \cos \alpha(z') \sin \beta(z')}{c^2 R(z')} \right. \\ & \left. \cdot \frac{\partial i(z', t - R(z')/c)}{\partial t} \right] dz' \quad (f) \\ & -\frac{1}{4\pi\epsilon_0} \hat{r} \left[\frac{\cos \theta - \cos \alpha(L') \cos \beta(L')}{c^2 R(L')} \right. \\ & \left. \cdot i(L', t - \frac{R(L')}{c}) \frac{dL'}{dt} \right] \quad (g) \\ & +\frac{1}{4\pi\epsilon_0} \hat{\theta} \left[\frac{\sin \theta + \cos \alpha(L') \sin \beta(L')}{c^2 R(L')} \right. \\ & \left. \cdot i(L', t - \frac{R(L')}{c}) \frac{dL'}{dt} \right] \quad (h) \end{aligned} \quad (9)$$

In equation (9), dL'/dt is the speed of the current wavefront as 'seen' by the observer at P, which is different from the real speed v . Also, from Fig. 1 we get $\cos \alpha(z') = -(z' - r \cos \theta) / R(z')$, $\cos \beta(z') = (r - z' \cos \theta) / R(z')$, and $\sin \beta(z') = z' \sin \theta / R(z')$. The lower limit of the time integral of the first term in (9), t_b , is the time at which

the return-stroke wavefront has reached the height z' for the first time, as 'seen' from the observation point. The last two terms of the expression (9) containing dL'/dt will have non-zero values only if there is a current discontinuity (non-zero current) at the wavefront. The apparent speed of the return stroke wavefront dL'/dt is

obtained from (1) as $\frac{dL'}{dt} = v \cdot \left[1 - \frac{v}{c} \cos \alpha(L') \right]^{-1}$ (see Equation (31) of [10]).

2.2 Magnetic Field

The magnetic field is given by $\bar{B} = \nabla \times \bar{A}$. For a vertical channel the magnetic field has only a horizontal component and it is given by (taking the curl of equation (3))

$$\begin{aligned} B(r, t) = & \\ & +\frac{1}{4\pi\epsilon_0 c^2} \hat{\phi} \int_0^{L(t)} \left[\frac{\sin \alpha(z')}{R^2(z')} i(z', t - \frac{R(z')}{c}) \right. \\ & \left. + \frac{\sin \alpha(z')}{cR(z')} \frac{\partial i(z', t - R(z')/c)}{\partial t} \right] dz' \quad (10) \\ & +\frac{1}{4\pi\epsilon_0 c^2} \hat{\phi} \frac{\sin \alpha(L')}{cR(L')} i(L', t - \frac{R(L')}{c}) \frac{dL'}{dt} \end{aligned}$$

where $\sin \alpha(z') = r \sin \theta / R(z')$

Equations (9) and (10) are valid for any return-stroke model, that is, for all time varying current and charge distributions on the channel. In the electric field expression (9) terms containing the factors R^{-3} , $c^{-1}R^{-2}$, and $c^{-2}R^{-1}$ constitute what is called the static component, the induction component, and the radiation component, respectively.

2.3 Image channel

A perfectly conducting plane at $z'=0$ is introduced to simulate the effect of earth. Using the image theory, we can replace this plane by an image channel carrying current in the same direction as the actual channel. The expression for the image channel can be easily obtained from (9) and (10) by replacing z' by $-z'$ wherever it appears. Note that the upper limit of integration for the image channel is L'' , which is less than L' for a field point above ground. Expression for L'' can be obtained from the expression for L' in (2) by replacing θ by $(180^\circ - \theta)$.

2.4 Fields at ground level

A common problem in lightning electromagnetics is to find the electric and magnetic fields at ground level from a lightning return-stroke, which is considered as a straight and vertical travelling wave antenna above ground. In this case $\theta=90^\circ$ and $\hat{\theta} = -\hat{z}$. The ground is assumed to be perfectly conducting. The effect of ground plane can be included by considering an image channel carrying an image current. The magnitude and direction of this image current is identical to the current in the channel at any given position and time, for an observer at ground level. In the field expression corresponding to the image channel the \hat{r} -directed components have the same magnitude, but opposite sign relative to the \hat{r} -directed components in (9). However, the field expression corresponding to the image channel contains $\hat{\theta}$ -directed components that are the same both in magnitude and sign as those in (9). Adding the contribution of the image channel to (9), we get the complete field expression as,

$$E_V(r,t) = \frac{+1}{2\pi\epsilon_0} \int_0^{L(t)} \frac{2-3\sin^2\alpha(z')}{R^3(z')} \int_{t_b}^t i(z',\tau - \frac{R(z')}{c}) d\tau dz' + \frac{+1}{2\pi\epsilon_0} \int_0^{L(t)} \frac{2-3\sin^2\alpha(z')}{cR^2(z')} i(z',t - \frac{R(z')}{c}) dz' \quad (11)$$

$$- \frac{1}{2\pi\epsilon_0} \int_0^{L(t)} \frac{\sin^2\alpha(z')}{c^2 R(z')} \frac{\partial i(z',t - R(z')/c)}{\partial t} dz'$$

$$- \frac{1}{2\pi\epsilon_0} \frac{\sin^2\alpha(L')}{c^2 R(L')} i(L',t - \frac{R(L')}{c}) \frac{dL'}{dt}$$

For a vertical channel the total magnetic field at ground level is horizontal, and is given by

$$B_\phi(r,t) = \frac{1}{2\pi\epsilon_0 c^2} \int_0^{L(t)} \left[\frac{\sin\alpha(z')}{R^2(z')} i(z',t - \frac{R(z')}{c}) + \frac{\sin\alpha(z')}{cR(z')} \frac{\partial i(z',t - R(z')/c)}{\partial t} \right] dz' \quad (12)$$

$$+ \frac{1}{2\pi\epsilon_0 c^2} \frac{\sin\alpha(L')}{cR(L')} i(L',t - \frac{R(L')}{c}) \frac{dL'}{dt}$$

The last term in equation (11) and the last term in equation (12) become zero if there is no current discontinuity at the propagating wavefront, i.e. if $i(L',t - R(L')/c) = 0$.

3. FIELDS IN TERMS OF CURRENT AND CHARGE DENSITY DISTRIBUTION (THE CONTINUITY EQUATION APPROACH)

3.1 Electric field

The purpose here is to find an expression for electric field using both scalar potential and vector potential related by the continuity equation that define the relationship between the charge density and current locally. The continuity equation that relates the charge density and current locally, but at retarded time, is given by equation (A4) in Appendix. As discussed in Appendix, in equation (A4), the partial differentiation of retarded current with respect to the source coordinate z' is carried out keeping the retarded time constant. That is, the dependence of $R(z')$ on z' is ignored while taking the partial derivative.

The return-stroke starts from the ground level ($z'=0$). To satisfy the continuity equation (A4) at $z'=0$, a point charge $Q(t-r/c)$ is required at $z'=0$ as the source for the current emerging from $z'=0$. This stationary point charge is given by,

$$Q(t-r/c) = - \int_{r/c}^t i(0,\tau - r/c) d\tau \quad (13)$$

The scalar potential from the whole lightning channel is given by

$$\phi(r,t) = \frac{1}{4\pi\epsilon_0} \frac{Q(t-r/c)}{r} + \frac{1}{4\pi\epsilon_0} \int_0^{L(t)} \frac{1}{R(z')} \rho^*(z',t - R(z')/c) dz' \quad (14)$$

It can be shown analytically that the expressions for scalar potentials in the two approaches, equation (14) and (8), are equivalent [3]. The electric field can be obtained from equation (4). Using the spherical coordinate system centered at the starting point of the return stroke at ground (Fig. 1) and ignoring the presence of ground for the moment, the negative gradient of the scalar potential $-\nabla\phi$ and the negative time derivative of the vector potential $-\partial\bar{A}/\partial t$ can be found as described below. Taking the gradient of (14), $-\nabla\phi$, we get equation (15):

$$\begin{aligned}
 -4\pi\epsilon_0\nabla\phi = & \\
 -\hat{r}\frac{\partial}{\partial r}\frac{Q(t-r/c)}{r} & \\
 -\hat{r}\frac{\partial}{\partial r}\int_0^{L(t)}\frac{\rho^*(z',t-R(z')/c)}{R(z')}dz' & \quad (15) \\
 -\hat{\theta}\frac{1}{r}\frac{\partial}{\partial\theta}\int_0^{L(t)}\frac{\rho^*(z',t-R(z')/c)}{R(z')}dz' &
 \end{aligned}$$

Note that the first term of equation (15) is independent of the spatial coordinate θ . The maximum length of the channel $L(t)$, as seen from the field point, is a function of r , θ , and t . The distance to the field point from the differential channel segment $R(z')$ is a function of both r and θ , (equations (A8)), and its spatial derivatives are given by

$$\begin{aligned}
 \frac{dR(z')}{dr} &= \frac{r-z'\cos\theta}{R(z')} \\
 \frac{dR(z')}{d\theta} &= \frac{rz'\sin\theta}{R(z')} \quad (16)
 \end{aligned}$$

Carrying out the differentiation of the second and third terms in equation (15) and using equations (16), we obtain the following expression

$$\begin{aligned}
 -4\pi\epsilon_0\nabla\phi = & \\
 +\hat{r}\int_0^{L(t)}\left[\frac{r-z'\cos\theta}{R^3(z')}\rho^*(z',t-R(z')/c)\right. & \\
 \left.+\frac{r-z'\cos\theta}{cR^2(z')}\frac{\partial\rho^*(z',t-R(z')/c)}{\partial t}\right]dz' & \\
 +\hat{\theta}\int_0^{L(t)}\left[\frac{z'\sin\theta}{R^3(z')}\rho^*(z',t-R(z')/c)\right. & \\
 \left.+\frac{z'\sin\theta}{cR^2(z')}\frac{\partial\rho^*(z',t-R(z')/c)}{\partial t}\right]dz' & \quad (17) \\
 -\hat{r}\frac{\rho^*(L',t-R(L')/c)}{R(L')}\frac{\partial L'}{\partial r} & \\
 -\hat{\theta}\frac{\rho^*(L',t-R(L')/c)}{rR(L')}\frac{\partial L'}{\partial\theta} -\hat{r}\frac{\partial}{\partial r}\frac{Q(t-r/c)}{r} &
 \end{aligned}$$

The time derivative of vector potential (3) is given by,

$$\begin{aligned}
 -4\pi\epsilon_0\frac{\partial\bar{A}}{\partial t} = & \\
 -\hat{z}\int_0^{L(t)}\frac{1}{c^2R(z')}\frac{\partial i(z',t-R(z')/c)}{\partial t}dz' & \quad (18) \\
 -\hat{z}\frac{i(L',t-R(L')/c)}{c^2R(L')}\frac{dL'}{dt} &
 \end{aligned}$$

$$\text{where } \hat{z} = \hat{r}\cos\theta - \hat{\theta}\sin\theta \quad (19)$$

The general expression for electric field at a field point can be found by combining equations (17), (18) and (19), and is given below.

$$\begin{aligned}
 \bar{E}(r,\theta,t) = & \\
 +\frac{1}{4\pi\epsilon_0}\hat{r}\int_0^{L(t)}\frac{\cos\beta(z')}{R^2(z')}\rho^*(z',t-\frac{R(z')}{c})dz' & \quad (a) \\
 +\frac{1}{4\pi\epsilon_0}\hat{r}\int_0^{L(t)}\frac{\cos\beta(z')}{cR(z')}\frac{\partial\rho^*(z',t-R(z')/c)}{\partial t}dz' & \quad (b) \\
 -\frac{1}{4\pi\epsilon_0}\hat{r}\int_0^{L(t)}\frac{\cos\theta}{c^2R(z')}\frac{\partial i(z',t-R(z')/c)}{\partial t}dz' & \quad (c) \\
 +\frac{1}{4\pi\epsilon_0}\hat{\theta}\int_0^{L(t)}\frac{\sin\beta(z')}{R^2(z')}\rho^*(z',t-\frac{R(z')}{c})dz' & \quad (d) \\
 +\frac{1}{4\pi\epsilon_0}\hat{\theta}\int_0^{L(t)}\frac{\sin\beta(z')}{cR(z')}\frac{\partial\rho^*(z',t-R(z')/c)}{\partial t}dz' & \quad (e) \\
 +\frac{1}{4\pi\epsilon_0}\hat{\theta}\int_0^{L(t)}\frac{\sin\theta}{c^2R(z')}\frac{\partial i(z',t-R(z')/c)}{\partial t}dz' & \quad (f) \\
 +\frac{1}{4\pi\epsilon_0}\hat{r}\frac{\cos\beta(L')}{cR(L')}\rho^*(L',t-\frac{R(L')}{c})\frac{dL'(t)}{dt} & \quad (g) \\
 -\frac{1}{4\pi\epsilon_0}\hat{r}\frac{\cos\theta}{c^2R(L')}\frac{\partial i(L',t-\frac{R(L')}{c})}{\partial t}\frac{dL'(t)}{dt} & \quad (h) \\
 +\frac{1}{4\pi\epsilon_0}\hat{\theta}\frac{\sin\beta(L')}{cR(L')}\rho^*(L',t-\frac{R(L')}{c})\frac{dL'(t)}{dt} & \quad (i) \\
 +\frac{1}{4\pi\epsilon_0}\hat{\theta}\frac{\sin\theta}{c^2R(L')}\frac{\partial i(L',t-\frac{R(L')}{c})}{\partial t}\frac{dL'(t)}{dt} & \quad (j) \\
 +\frac{1}{4\pi\epsilon_0}\hat{r}\frac{1}{r^2}Q(t-r/c) & \quad (k) \\
 +\frac{1}{4\pi\epsilon_0}\hat{r}\frac{1}{rc}\frac{dQ(t-r/c)}{dt} & \quad (l)
 \end{aligned} \quad (20)$$

where, $\cos\beta(z')=(r-z'\cos\theta)/R(z')$, $\sin\beta(z')=z'\sin\theta/R(z')$, and Q is given by (13). Note that by definition, the

current and charge density in (20) are related by the local continuity equation (A4).

The magnetic field expression using this approach is identical to equation (10) since it is completely determined by the vector potential.

In the electric field expression (20) terms containing the factors R^{-3} , $c^{-1}R^{-2}$, and $c^{-2}R^{-1}$ (note that the factors $\cos\beta(z')$ and $\sin\beta(z')$ contain R^{-1}) constitute what is called the static component, the induction component, and the radiation component, respectively. However, the static/induction/radiation components in (20) are not equal to their corresponding components in (9). To give an example, sum of the static terms (a), (d) and (k) in (20) is not equal to the sum of the static terms (a) and (d) in (9). However, it has been proved both analytically and numerically in [3,4] that total fields represented by equation (9) and (20) are equal. That is, even though the individual field components described as static, induction and radiation are not the same in (9) and (20), the total field is the same. More on the non-uniqueness of field components are presented at a later section.

3.2 Image channel

A perfectly conducting plane at $z'=0$ is introduced to simulate the effect of earth. Using the image theory, we can replace this plane by an image channel carrying current in the same direction as the actual channel. The expression for the image channel can be easily obtained from (20) by replacing z' by $-z'$, ρ by $-\rho$, and Q by $-Q$, wherever they appear. Note that the upper limit of integration for the image channel is L'' , which is less than L' for a field point above ground. As discussed before, expression for L'' can be obtained from the expression for L' given by (3) by replacing θ by $(180^\circ - \theta)$.

3.3 Electric Field at ground level

We are interested in the return stroke field at ground level. For this case, $\theta=90^\circ$, and therefore $\cos \theta = 0$, $\sin \theta = 1$, and $\hat{\theta} = -\hat{z}$. The unit vector \hat{r} is now horizontal, pointing away from the channel. Writing out the equations for image channel and adding them to equation (20) for the case $\theta = 90^\circ$, we get the expression for E-field, as below.

$$\begin{aligned}
 E_v(r,t) = & \\
 & \frac{-1}{2\pi\epsilon_0} \int_0^{L'(t)} \frac{z'}{R^3(z')} \rho^*(z',t-R(z')/c) dz' \\
 & \frac{-1}{2\pi\epsilon_0} \int_0^{L'(t)} \frac{z'}{cR^2(z')} \frac{\partial \rho^*(z',t-R(z')/c)}{\partial t} dz' \\
 & \frac{-1}{2\pi\epsilon_0} \int_0^{L'(t)} \frac{1}{c^2R(z')} \frac{\partial i(z',t-R(z')/c)}{\partial t} dz' \tag{21} \\
 & \frac{-1}{2\pi\epsilon_0} \frac{L'(t)}{cR^2(L')} \rho^*(L',t-R(L')/c) \frac{dL'}{dt} \\
 & \frac{-1}{2\pi\epsilon_0} \frac{1}{c^2R(L')} i(L',t-R(L')/c) \frac{dL'}{dt}
 \end{aligned}$$

By analogy with equation (11), the first term of equation (21) can be considered as representing the electrostatic field (R^{-3} dependence), the sum of second and fourth terms as representing the induction field ($c^{-1}R^{-2}$ dependence), and the sum of third and last terms as representing the radiation field ($c^{-2}R^{-1}$ dependence). It appears that the electrostatic, induction, and radiation terms (except for the last two terms associated with the wavefront) in (21) can also be identified as containing z' times line charge density (charge), z' times time derivative of line charge density (time derivative of charge) or current, and derivative of current, respectively. If there is no current or charge discontinuity at the wavefront, the last two terms vanish.

3.4 Non-uniqueness of field components

Thottappillil and Rakov [3, 4] discusses the non-uniqueness of individual field components, represented as static, induction and radiation, in the field expression (9) and (20). The total fields given by equations (9) and (20) are identical. In equation (20), the electrostatic and induction terms are given completely by the gradient of the scalar potential, while the radiation term is completely given by the time derivative of the vector potential. In contrast, in equation (9), both the gradient of the scalar potential and the time derivative of the vector potential contribute to the radiation field term. The electrostatic (R^{-3} dependence), induction ($c^{-1}R^{-2}$ dependence), and radiation ($c^{-2}R^{-1}$ dependence) terms in (9) are different from the corresponding terms in (20). The difference is considerable at very close distance to the channel (e.g., 50 m) and almost negligible at far away from the

channel (e.g., 100 km). Calculations with the transmission line model shows that very close to the channel, the electrostatic term (R^{-3} dependence) in equation (11) is larger than its counterpart in equation (21). However, if we use the electrostatic approximation (assume infinite field propagation speed), the electrostatic terms in equations (11) and (21) will be equivalent.

The analysis clearly shows that, even though the total electric field from a current or charge distribution is unique, the division of total electric field in the time domain into so-called electrostatic (R^{-3} dependence), induction ($c^{-1}R^{-2}$ dependence), and radiation ($c^{-2}R^{-1}$ dependence) components is not unique. Note that in the Lorentz condition technique all field components are expressed in terms of current, while in the continuity equation technique both current and charge density are involved. We get the same Poynting vector whether we calculate it from equation pairs (9) and (10) or (20) and (10), since the total electric fields given by (9) and (20) are the same. In fact [3] show how equation (9) can be analytically derived from equation (20).

4 FIELDS IN TERMS OF APPARENT CHARGE DENSITY DISTRIBUTION

It is possible to derive an electric field expression completely in terms of apparent charge density or charge density as 'seen' by the remote observer as first shown by [5]. The relationship between apparent charge density and the local charge density in retarded time are established earlier in equation (A13).

The general expression (20) in terms of current can be taken as a starting point. The procedure presented in [5] for the special case of fields at ground level is generalised for fields at any point above ground and is as follows.

4.1 Relation between 'apparent charge density' and retarded current

The continuity equation relating the retarded charge density as 'seen' by the observer (apparent charge density) and retarded current at an arbitrary time t is given by equation (A6). The return-stroke front is assumed to start from ground level ($z'=0$) and to propagate upward with a constant speed v , reaching a height z' in a time z'/v . Taking the time integral from $z'/v+R(z')/c$ to t on both sides of (A6), noting that z' and t are independent variables, we obtain an expression for apparent charge density in terms of retarded current as

$$\rho(z', t - R(z')/c) = \frac{i(z', z'/v)}{v_a(z')} - \int_{z'/v+R(z')/c}^t \frac{\partial i(z', \tau - R(z')/c)}{\partial z'} d\tau \quad (22)$$

where $v_a(z')$ is the apparent speed of the front at z' as seen by a stationary observer at a distance r from the base of the channel and is given by

$$\frac{1}{v_a(z')} = - \frac{\partial}{\partial z'} \left(t - \frac{R(z')}{c} - \frac{z'}{v} \right) = \frac{1}{v} \cdot (1 - \frac{v}{c} \cos \alpha(z')) \quad (23)$$

Angle $\alpha(z')$ is defined in Fig. 1. Note that the first term of (22) represents the charge density at the wavefront when it has reached z' and is due to the extension of the front. Equation (22) defines the charge density distribution along the channel at any given time t as "seen" by a stationary observer at P at a distance r from the base of the channel (see Fig. 1). Equation (22) can be rewritten as

$$\rho(z', t - \frac{R(z')}{c}) = - \frac{d}{dz'} \int_{\frac{z'+R(z')}{v}}^t i(z', \tau - \frac{R(z')}{c}) d\tau \quad (24)$$

From (24), we find

$$\rho(z', t - \frac{R(z')}{c}) dz' = - d \left[\int_{\frac{z'+R(z')}{v}}^t i(z', \tau - \frac{R(z')}{c}) d\tau \right] \quad (25)$$

Further, multiplying both sides of (25) by dz' , we find

$$\frac{\partial \rho(z', t - R(z')/c)}{\partial t} dz' = - \frac{\partial i(z', t - R(z')/c)}{\partial z'} dz' = - di(z', t - R(z')/c) \quad (26)$$

Finally, taking the partial derivative with respect to time of (26), we obtain

$$\frac{\partial^2 \rho(z', t - R(z')/c)}{\partial t^2} dz' = - d \left(\frac{\partial i(z', t - R(z')/c)}{\partial t} \right) \quad (27)$$

In general, the lower limit of the integral in (24) and (25) is the time, $t_b(z')$, at which the current is "seen" to begin in the channel at z' by the observer and with this modification equation (25), along with (26) and (27) are valid for any lightning process. It is not necessary for

the return stroke speed to be constant if the lower limit of (25) is written as $t_b(z')$.

The remote differential electric field at ground due to a vertical, current carrying element dz' above a perfectly conducting earth is given by the integrand of (9). Each term of integrand of (9) can be represented, omitting $1/(4\pi\epsilon_0)$, by

$$df_1(z') f_2(z',t) = d[f_1(z') f_2(z',t)] - f_1(z') df_2(z',t) \quad (28)$$

where $f_2(z',t)$ is the current integral, current or the current derivative and the total differential $df_1(z')$ is any one of the remaining factors, and given by equations (29) – (34) below.

$$d\left(\frac{r - z' \cos \theta}{R^3(z')}\right) = -\left(\frac{\cos \theta - 3 \cos \alpha(z') \cos \beta(z')}{R^3(z')}\right) dz' \quad (29)$$

$$d\left(\frac{3}{2} \frac{r - z' \cos \theta}{cR^2(z')} + \frac{1}{2} \frac{\cot \theta}{cr} \tan^{-1} \frac{z' - r \cos \theta}{r \sin \theta}\right) = -\left(\frac{\cos \theta - 3 \cos \alpha(z') \cos \beta(z')}{cR^2(z')}\right) dz' \quad (30)$$

$$d\left(\frac{r - z' \cos \theta}{c^2 R(z')}\right) = -\left(\frac{\cos \theta - \cos \alpha(z') \cos \beta(z')}{c^2 R(z')}\right) dz' \quad (31)$$

$$d\left(\frac{z' \sin \theta}{R^3(z')}\right) = \frac{\sin \theta + 3 \cos \alpha(z') \sin \beta(z')}{R^3(z')} dz' \quad (32)$$

$$d\left(\frac{3}{2} \frac{z' \sin \theta}{cR^2(z')} - \frac{1}{2} \frac{1}{cr} \tan^{-1} \frac{z' - r \cos \theta}{r \sin \theta}\right) = \frac{\sin \theta + 3 \cos \alpha(z') \sin \beta(z')}{cR^2(z')} dz' \quad (33)$$

$$d\left(\frac{z' \sin \theta}{c^2 R(z')}\right) = \frac{\sin \theta + \cos \alpha(z') \sin \beta(z')}{c^2 R(z')} dz' \quad (34)$$

Function $df_2(z')$ can be written in terms of charge density using (25), (26), and (27). Using equations (25) - (34) in equation (9), and carrying out the integration between the limits 0 and $L'(t)$, we get the general expression for electric field at an elevation as Equation (35). In (35), $\cos \alpha(z') = -(z' - r \cos \theta)/R(z')$, $\sin \alpha(z') = r \sin \theta / R(z')$, $\cos \beta(z') = (r - z' \cos \theta)/R(z')$, $\sin \beta(z') = z' \sin \theta / R(z')$, and Q is given by (13). Note also that, $\tan^{-1}(-\cot(\alpha(z'))) = \pi/2 + \alpha(z')$. Expression (35) does not include the effect of the ground plane.

In Equations (35) and (9), the terms analytically equivalent are shown in Table 1.

Table 1. Terms analytically equivalent in the electric field expressions (35) and (9).

Terms in eq. (35)	Equivalent terms in eq. (9)	Comments
(a)+(d)	(a)	static component along \hat{r}
(b)+(e)+(g)	(b)	induction component along \hat{r}
(c)+(f)+(h)	(c)	radiation component along \hat{r}
(i)	(d)	static component along $\hat{\theta}$
(j)+(l)+(m)	(e)	induction component along $\hat{\theta}$
(k)+(n)	(f)	radiation component along $\hat{\theta}$
(o)	(g)	radiation component along \hat{r} due to source discontinuity at return-stroke wave front
(p)	(h)	radiation component along $\hat{\theta}$ due to source discontinuity at return-stroke wave front

It is also possible to derive a general expression for magnetic field in terms of apparent charge, starting from (10). As before, each term of integrand of (10) can be represented, omitting $1/(4\pi\epsilon_0 c^2)$, by equation (28), where $f_2(z',t)$ is the current or the current derivative and the total differential $df_1(z')$ is any one of the remaining factors and is given by Equations (36) – (37).

$$\begin{aligned}
 \bar{E}(r, \theta, t) = & \\
 + \frac{1}{4\pi\epsilon_0} \hat{r} \int_0^{L'(t)} \frac{\cos \beta(z')}{R^2(z')} \rho(z', t - R(z')/c) dz' & \quad (a) \\
 + \frac{1}{4\pi\epsilon_0} \hat{r} \int_0^{L'(t)} \left[\frac{3 \cos \beta(z')}{2 cR(z')} + \frac{1 \cot \theta}{2 cr} \tan^{-1}(-\cot \alpha(z')) \right] \frac{\partial \rho(z', t - R(z')/c)}{\partial t} dz' & \quad (b) \\
 + \frac{1}{4\pi\epsilon_0} \hat{r} \int_0^{L'(t)} \frac{\cos \beta(z')}{c^2} \frac{\partial^2 \rho(z', t - R(z')/c)}{\partial t^2} dz' & \quad (c) \\
 + \frac{1}{4\pi\epsilon_0} \hat{r} \frac{1}{r^2} Q(t - r/c) & \quad (d) \\
 + \frac{1}{4\pi\epsilon_0} \hat{r} \left[\frac{3}{2} \frac{1}{cr} + \frac{1}{2} \cot \theta \frac{\tan^{-1}(-\cot \theta)}{cr} \right] \frac{\partial Q(t - r/c)}{\partial t} & \quad (e) \\
 + \frac{1}{4\pi\epsilon_0} \hat{r} \frac{1}{c^2} \frac{\partial^2 Q(t - r/c)}{\partial t^2} & \quad (f) \\
 + \frac{1}{4\pi\epsilon_0} \hat{r} \left[\frac{3 \cos \beta(L')}{2 cR(L')} + \frac{1 \cot \theta}{2 cr} \tan^{-1}(-\cot \alpha(L')) \right] \rho(L', t - R(L')/c) \frac{dL'(t)}{dt} & \quad (g) \quad (35) \\
 + \frac{1}{4\pi\epsilon_0} \hat{r} \frac{\cos \beta(L')}{c^2} \frac{\partial}{\partial t} \left[\rho(L', t - R(L')/c) \frac{dL'(t)}{dt} \right] & \quad (h) \\
 + \frac{1}{4\pi\epsilon_0} \hat{\theta} \int_0^{L'(t)} \frac{\sin \beta(z')}{R^2(z')} \rho(z', t - R(z')/c) dz' & \quad (i) \\
 + \frac{1}{4\pi\epsilon_0} \hat{\theta} \int_0^{L'(t)} \left[\frac{3 \sin \beta(z')}{2 cR(z')} - \frac{1}{2} \frac{1}{cr} \tan^{-1}(-\cot \alpha(z')) \right] \frac{\partial \rho(z', t - R(z')/c)}{\partial t} dz' & \quad (j) \\
 + \frac{1}{4\pi\epsilon_0} \hat{\theta} \int_0^{L'(t)} \frac{\sin \beta(z')}{c^2} \frac{\partial^2 \rho(z', t - R(z')/c)}{\partial t^2} dz' & \quad (k) \\
 - \frac{1}{4\pi\epsilon_0} \hat{\theta} \frac{1}{2} \frac{\tan^{-1}(-\cot \theta)}{cr} \frac{\partial Q(t - r/c)}{\partial t} & \quad (l) \\
 + \frac{1}{4\pi\epsilon_0} \hat{\theta} \left[\frac{3 \sin \beta(L')}{2 cR(L')} - \frac{1}{2} \frac{1}{cr} \tan^{-1}(-\cot \alpha(L')) \right] \rho(L', t - R(L')/c) \frac{dL'(t)}{dt} & \quad (m) \\
 + \frac{1}{4\pi\epsilon_0} \hat{\theta} \frac{\sin \beta(L')}{c^2} \frac{\partial}{\partial t} \left[\rho(L', t - R(L')/c) \frac{dL'(t)}{dt} \right] & \quad (n) \\
 - \frac{1}{4\pi\epsilon_0} \hat{r} \frac{\cos \theta - \cos \alpha(L') \cos \beta(L')}{c^2 R(L')} \rho(L', t - \frac{R(L')}{c}) \left(\frac{dL'}{dt} \right)^2 & \quad (o) \\
 + \frac{1}{4\pi\epsilon_0} \hat{\theta} \frac{\sin \theta + \cos \alpha(L') \sin \beta(L')}{c^2 R(L')} \rho(L', t - \frac{R(L')}{c}) \left(\frac{dL'}{dt} \right)^2 & \quad (p)
 \end{aligned}$$

$$d\left(\frac{1}{c} \tan^{-1}\left(\frac{z'-r \cos \theta}{r \sin \theta}\right)\right) = \frac{r \sin \theta}{cR^2(z')} dz' \quad (36)$$

$$d\left(\frac{z'-r \cos \theta}{r \sin \theta} \frac{1}{R(z')}\right) = \frac{r \sin \theta}{R^3(z')} dz' \quad (37)$$

Function $df_2(z')$ can be written in terms of charge density using (26) and (27). Using equations (26) - (28) and (36) - (37) in equation (10), and carrying out the integration between the limits 0 and $L'(t)$, we get the general expression for magnetic field at an elevation as in (38).

$$B(r, \theta, t) =$$

$$\frac{1}{4\pi\epsilon_0 c^2} \hat{\phi} \int_0^{L'(t)} \left[\frac{1}{r \sin \theta} \frac{z'-r \cos \theta}{R(z')} \frac{\partial \rho(z', t - R(z')/c)}{\partial t} \right] dz' \quad (a)$$

$$+ \frac{1}{4\pi\epsilon_0 c^2} \hat{\phi} \int_0^{L'(t)} \left[\frac{1}{r \sin \theta} \frac{z'-r \cos \theta}{R(z')} \frac{\partial \rho^2(z', t - R(z')/c)}{\partial t^2} \right] dz' \quad (b)$$

$$+ \frac{1}{4\pi\epsilon_0 c^2} \hat{\phi} \frac{1}{r \sin \theta} \frac{L'(t) - r \cos \theta}{R(L')} \cdot \rho(L', t - R(L')/c) \frac{dL'(t)}{dt} \quad (c)$$

$$+ \frac{1}{4\pi\epsilon_0 c^2} \hat{\phi} \frac{\cot \theta}{r} \frac{\partial Q(t - r/c)}{\partial t} \quad (d)$$

$$+ \frac{1}{4\pi\epsilon_0 c^2} \hat{\phi} \frac{1}{c} \tan^{-1} \frac{L'(t) - r \cos \theta}{r \sin \theta} \cdot \frac{\partial}{\partial t} \left[\rho(L', t - \frac{R(L')}{c}) \frac{dL'(t)}{dt} \right] \quad (e)$$

$$+ \frac{1}{4\pi\epsilon_0 c^2} \hat{\phi} \frac{1}{c} \tan^{-1}(-\cot \theta) \frac{\partial^2 Q(t - r/c)}{\partial t^2} \quad (f)$$

$$+ \frac{1}{4\pi\epsilon_0 c^2} \hat{\phi} \frac{\sin \alpha(L')}{cR(L')} \rho(L', t - \frac{R(L')}{c}) \left(\frac{dL'}{dt} \right)^2 \quad (g)$$

$$(38)$$

In equation (38), sum of the terms marked as (a), (c), and (d) corresponds to magnetostatic field component which is analytically equivalent to the magnetostatic term (first term) of (10), sum of the terms marked as (b), (e), and (f) corresponds to the radiation term which is analytically equivalent to the radiation term (second term) of (10), and term marked as (g) is the radiation term corresponding to current discontinuity at the propagating wavefront which is analytically equivalent

to the last term of (10). Equation (38) is new (not found in previous literature). In field equations (35) and (38), the apparent charge density is related to the current by equation (A6).

4.2 Image channel

A perfectly conducting plane at $z'=0$ can be introduced to simulate the effect of earth. Using the image theory, we can replace this plane by an image channel carrying current in the same direction as the actual channel. The expression for the image channel can be easily obtained from (35) and (38) by replacing z' by $-z'$, ρ by $-\rho$, and Q by $-Q$, wherever they appear. Note that the upper limit of integration for the image channel is L'' , which is less than L' for a field point above ground. As discussed before, expression for L'' can be obtained from the expression for L' in (2) by replacing θ by $(180-\theta)$.

4.3 Fields at ground level

We are interested in the return stroke field at ground level. For this case, $\theta=90^\circ$, and therefore $\cos \theta = 0$, $\sin \theta = 1$, and $\hat{\theta} = -\hat{z}$. The unit vector \hat{r} is now horizontal, pointing away from the channel. Writing out the equations for image channel and adding them to equation (35) for the case $\theta = 90^\circ$, we see that all the \hat{r} terms cancel each other and the expression for E-field has only vertically directed components, as below (e.g., [5]) in Equation (39).

$$E_v(r, t) = -\frac{1}{2\pi \epsilon_0} \hat{z} \int_0^{L'(t)} \frac{z'}{R^3(z')} \rho(z', t - \frac{R(z')}{c}) dz'$$

$$- \frac{1}{2\pi \epsilon_0} \hat{z} \int_0^{L'(t)} \left(\frac{\frac{3}{2} \frac{z'}{cR^2(z')} - \frac{1}{2} \frac{\tan^{-1}(z'/r)}{cr}}{\frac{1}{2} \frac{\tan^{-1}(z'/r)}{cr}} \right) \frac{\partial \rho(z', t - R(z')/c)}{\partial t} dz'$$

$$- \frac{1}{2\pi \epsilon_0} \hat{z} \int_0^{L'(t)} \frac{z'}{c^2 R(z')} \frac{\partial^2 \rho(z', t - R(z')/c)}{\partial t^2} dz'$$

$$- \frac{1}{2\pi \epsilon_0} \hat{z} \left(\frac{\frac{3}{2} \frac{L'(t)}{cR^2(L')} - \frac{1}{2} \frac{\tan^{-1}(L'(t)/r)}{cr}}{\frac{1}{2} \frac{\tan^{-1}(L'(t)/r)}{cr}} \right) \rho(L', t - \frac{R(L')}{c}) \frac{dL'(t)}{dt}$$

$$- \frac{1}{2\pi \epsilon_0} \hat{z} \frac{L'(t)}{c^2 R(L')} \frac{\partial}{\partial t} \left[\rho(L', t - \frac{R(L')}{c}) \frac{dL'(t)}{dt} \right]$$

$$- \frac{1}{2\pi \epsilon_0} \hat{z} \frac{r^2}{c^2 R^3(L')} \rho(L', t - \frac{R(L')}{c}) \left(\frac{dL'}{dt} \right)^2 \quad (39)$$

Similarly the magnetic field at the ground level is given by [5], as in (40).

$$\begin{aligned}
 B_\phi(r,t) = & \frac{1}{2\pi \epsilon_0 c^2} \int_0^{L(t)} \frac{1}{r} \frac{z'}{R(z')} \frac{\partial \rho(z',t-R(z')/c)}{\partial t} dz' \\
 & + \frac{1}{2\pi \epsilon_0 c^2} \int_0^{L(t)} \frac{1}{c} \tan^{-1}\left(\frac{z'}{r}\right) \frac{\partial^2 \rho(z',t-R(z')/c)}{\partial t^2} dz' \\
 & + \frac{1}{2\pi \epsilon_0 c^2} \frac{1}{r} \frac{L'(t)}{R(L')} \rho(L'(t), \frac{L'(t)}{v}) \frac{dL'(t)}{dt} \quad (40) \\
 & + \frac{1}{2\pi \epsilon_0 c^2} \frac{1}{c} \tan^{-1}\left(\frac{L'(t)}{r}\right) \\
 & \quad \cdot \frac{\partial}{\partial t} \left[\rho(L',t-\frac{R(L')}{c}) \frac{dL'(t)}{dt} \right] \\
 & + \frac{1}{2\pi \epsilon_0 c^2} \frac{r}{cR^2(L')} \rho(L',t-\frac{R(L')}{c}) \left(\frac{dL'(t)}{dt} \right)^2
 \end{aligned}$$

5 FIELDS AT AN ELEVATION FROM RETURN STROKES

Numerical calculation of fields at different elevation and distance from the lightning return stroke is presented in this section. The equivalence between the electric field expressions derived using the Lorentz condition technique (dipole technique) and the continuity equation technique (monopole technique) has been numerically established in [3, 4]. The main purpose of the calculations in this section is the verification of the equivalence between the general field expressions at an elevation using the current formulation and apparent charge formulation. Electric fields at different angles from the vertical, at different distances from channel-base and for different return stroke speeds are calculated using (9) and (35), including the images to take into account the effect of a perfectly conducting ground. Similarly, magnetic fields at different angles from the vertical, different distances from channel-base and different return stroke speeds are calculated using (10) and (38), including the images to take into account the effect of a perfectly conducting ground. The transmission line (TL) model of the return stroke is used for computations (For discussion of various return stroke models, see Chapter (12) in Rakov and Uman [11]).

5.1 Electric fields

Figs. 2-8 shows the electric fields above a perfectly conducting ground at distances 100 m, 1000 m, and 100 km from the channel base of the return stroke for various angles 10°, 30°, 60°, and 90° (ground level) with respect to vertical. Assumed return stroke speed is 1.5x10⁸ m/s for results presented in Figs. 2-4, 2.7x10⁸ m/s for results in Figs. 5-7, and 3x10⁸ m/s (speed of light; the upper-bound case) for results in Fig. 8. Electric fields for the speed of light were calculated using the simple exact expression derived in Thottappillil et al. [12, 13] given by

$$\bar{E}(r,\theta,t) = \hat{\theta} \frac{1}{2\pi\epsilon_0 cr \sin \theta} i(0,t-r/c) \quad (41)$$

For the case of TL model, equation (41) is equivalent to the sum of equation (9) and similar equation applicable for the image channel. The channel-base current used in all the calculations presented in this paper are that given by Nucci et al. [14], which has a peak of about 11 kA and maximum current rate of rise of 110 kA/μs, which are thought to be representative of subsequent return strokes. The r-component of the electric field at a distance of 100 km is very small and hence not presented.

The vertical and horizontal E-fields (E_v and E_H , respectively) can be obtained from the calculated r-component and θ -component of the E-fields (E_r and E_θ , respectively) as,

$$\begin{aligned}
 E_v &= E_r \cos \theta - E_\theta \sin \theta \\
 E_H &= E_r \sin \theta + E_\theta \cos \theta
 \end{aligned} \quad (42)$$

In Figs. 2 -7, fields calculated using the current formulation (solid line) is the same as that calculated using the apparent charge formulation (dotted line), verifying the equivalence between equations (9) and (35). Table 2 summarizes the peak electric fields as a function of angle from the vertical, return stroke speed, and distance from channel-base. At close distances (100 m and 1000 m), both the r-component and θ -component have the largest peak value at small angles for all return stroke speeds. However, at a far distance of 100 km, where the field is almost entirely due to radiation, the r-component is negligible and the θ -component has the largest peak value at 90° at lower speeds ($v=1.5 \times 10^8$ m/s) and the smallest peak value at 90° for the limiting speed equal to the speed of light. At a speed of 2.7x10⁸ m/s, the maximum radiation is at an angle between 10° and 90°. The existence of a critical angle lower than 90° at which the far radiated field attains a maximum has been discussed in Krider

[15], Thottappillil et al. [12], and Rakov and Tuni [16]. Also, at closer distances (100 m and 1000 m), the peak electric fields decreases with increasing return stroke speed whereas at far distance there is an opposite trend in which the far fields increase dramatically with increasing speed. The linear dependence of the far field peak on the speed of the return stroke is valid only for $\theta=90^\circ$. At other angles, the dependence of the far field peak on the speed is complicated and much stronger than the linear dependence would suggest. For example, at 10° , changing the speed from $v=0.5c$ to $v=c$ increases the field peak by a factor of 50.

formulation, dotted line – apparent charge formulation. The two types of lines (fields for two formulations) are indistinguishable in the plot. Blue – 10° , Red – 30° , Green – 60° , Black – 90° (angle is measured with respect to vertical). Time in μs on the x-axis and E-field in V/m on the y-axis.

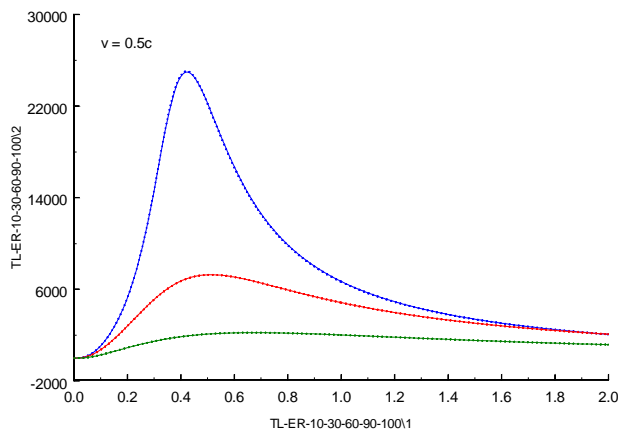


Figure 2a: The r-component of E-field predicted by the TL model for return stroke speed $v = 0.5c$, above perfectly conducting ground at a distance of 100 m from channel-base. Solid line – current formulation, dotted line – apparent charge formulation. The two types of lines (fields for two formulations) are indistinguishable in the plot. Blue – 10° , Red – 30° , Green – 60° . The r-component is zero at 90° and hence not shown (angle is measured with respect to vertical). Time in μs on the x-axis and E-field in V/m on the y-axis.

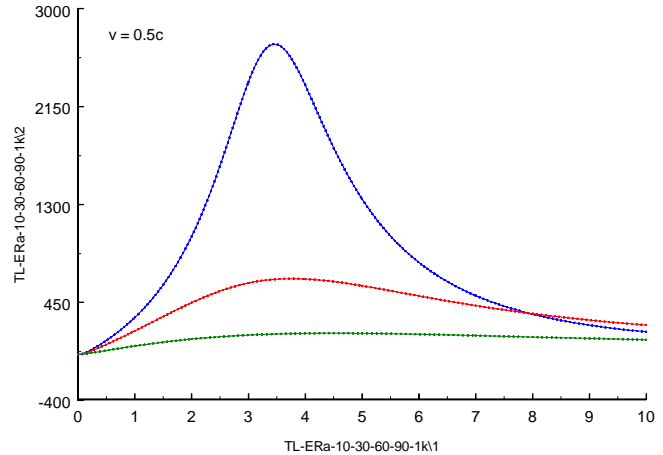


Figure 3a: The r-component of E-field predicted by the TL model for return stroke speed $v = 0.5c$, above perfectly conducting ground at a distance of 1000 m from channel-base. Solid line - current formulation, dotted line – apparent charge formulation. The two types of lines (fields for two formulations) are indistinguishable in the plot. Blue – 10° , Red – 30° , Green – 60° . The r-component is zero at 90° and hence not shown (angle is measured with respect to vertical). Time in μs on the x-axis and E-field in V/m on the y-axis.

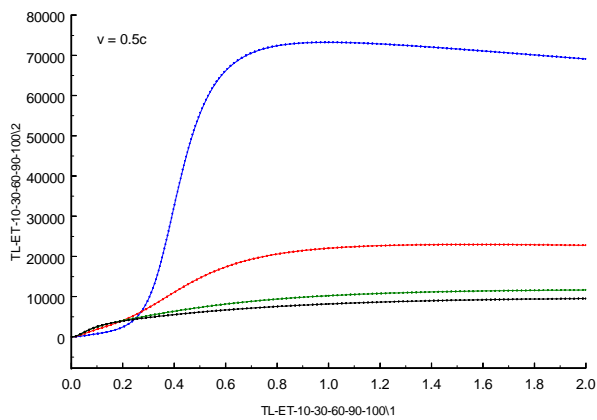


Figure 2b: The θ -component of E-field predicted by the TL model for return stroke speed $v = 0.5c$, above perfectly conducting ground at a distance of 100 m from channel-base. Solid line – current

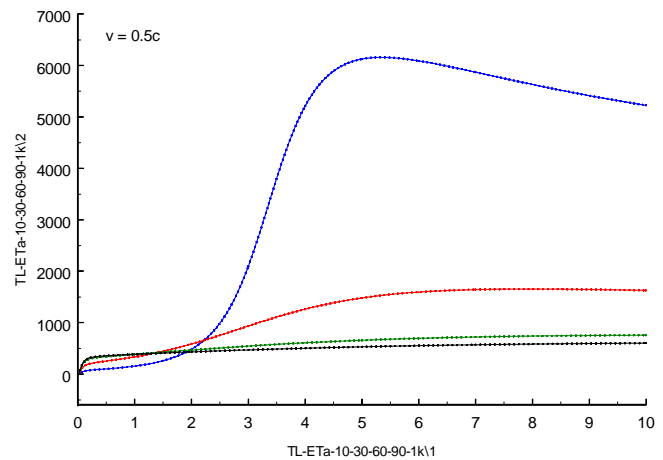


Figure 3b: The θ -component of E-field predicted by the TL model for return stroke speed $v = 0.5c$, above perfectly conducting ground at a distance of 1000 m from channel-base. Solid line - current formulation, dotted line – apparent charge formulation. The two types of lines (fields for two formulations) are indistinguishable in the plot. Blue – 10° , Red – 30° , Green – 60° , Black – 90° (angle is measured with respect to vertical). Time in μs on the x-axis and E-field in V/m on the y-axis.

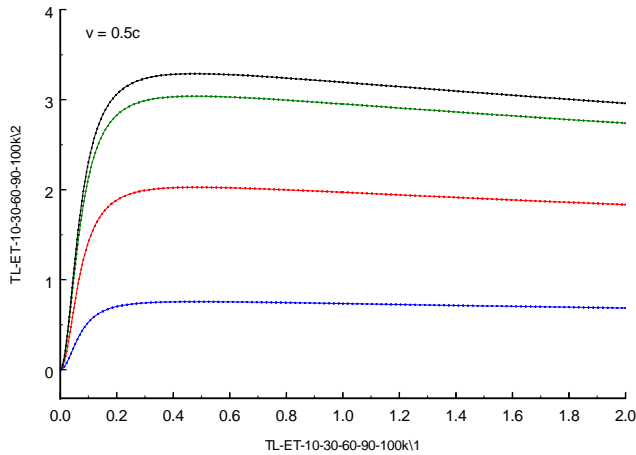


Figure 4: The θ -component of E-field predicted by the TL model for return stroke speed $v = 0.5c$, above perfectly conducting ground at a distance of 100 km from channel-base. Solid line - current formulation, dotted line - apparent charge formulation. The two types of lines (fields for two formulations) are indistinguishable in the plot. Blue - 10° , Red - 30° , Green - 60° , Black - 90° (angle is measured with respect to vertical). Time in μs on the x-axis and E-field in V/m on the y-axis.

Table 2a: Peak electric fields in V/m as a function of angle and return stroke speed at a distance of 100 m from channel-base as predicted by TL model.

Angle from Vertical	E _θ at 100 m			E _r at 100 m		
	v=0.5c Fig.2b.	v=0.9c Fig.5b	v=c Fig.8a	v=0.5c Fig.2a.	v=0.9c Fig.5a	v=c
10°	73300	41800	37828	25000	3500	0
30°	23000	14100	13137	7280	1030	0
60°	11700	7800	7585	2220	306	0
90°	9500	6700	6569	0	0	0

Table 2b: Peak electric fields in V/m as a function of angle and return stroke speed at a distance of 1000 m from channel-base as predicted by TL model.

Angle from Vertical	E _θ at 1000 m			E _r at 1000 m		
	v=0.5c Fig.3b.	v=0.9c Fig.6b	v=c Fig.8b	v=0.5c Fig.3a	v=0.9c Fig.6a	v=c
10°	6160	3900	3783	2690	617	0
30°	1656	1230	1314	657	121	0
60°	760	684	758	184	30	0
90°	603	605	657	0	0	0

Table 2c: Peak electric fields in V/m as a function of angle and return stroke speed at a distance of 100 km from channel-base as predicted by TL model.

Angle from Vertical	E _θ at 100 km			E _r at 100 km		
	v=0.5c Fig. 4	v=0.9c Fig. 7	v=c Fig. 8c	v=0.5c	v=0.9c	v=c
10°	0.76	4.9	38	-	-	0
30°	2.0	7.6	13	-	-	0
60°	3.0	6.4	7.6	-	-	0
90°	3.3	5.9	6.6	0	0	0

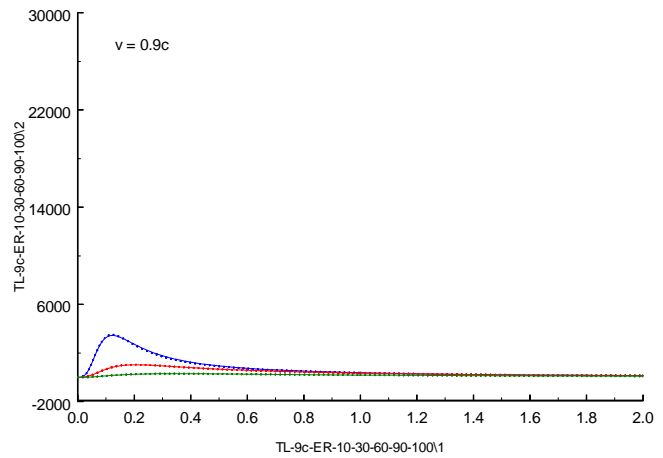


Figure 5a: The r-component of E-field predicted by the TL model for return stroke speed $v = 0.9c$, above perfectly conducting ground at a distance of 100 m from channel-base. Other details are as in the caption of Fig. 2a. Note the substantial reduction in the r-component field with increased speed.

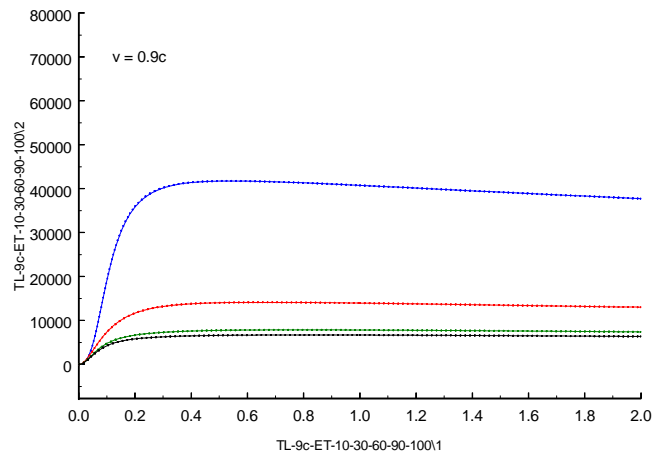


Figure 5b: The θ -component of E-field predicted by the TL model for return stroke speed $v = 0.9c$, above perfectly conducting ground at a distance of 100 m from channel-base. Other details are as in the caption of Fig. 2b.

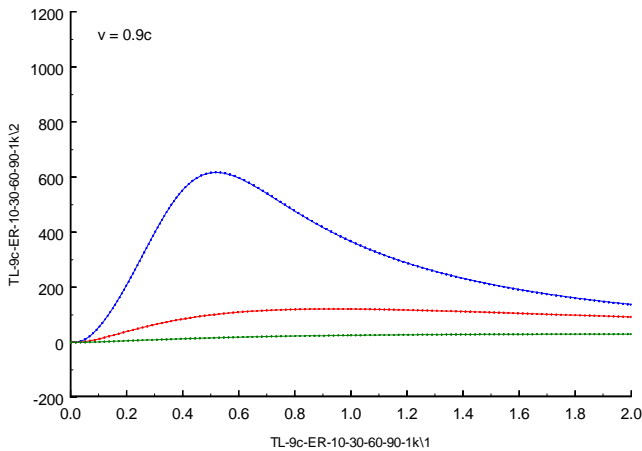


Figure 6a: The r-component of E-field predicted by the TL model for return stroke speed $v = 0.9c$, above perfectly conducting ground at a distance of 1000 m from channel-base. Other details are as in the caption of Fig. 3a.

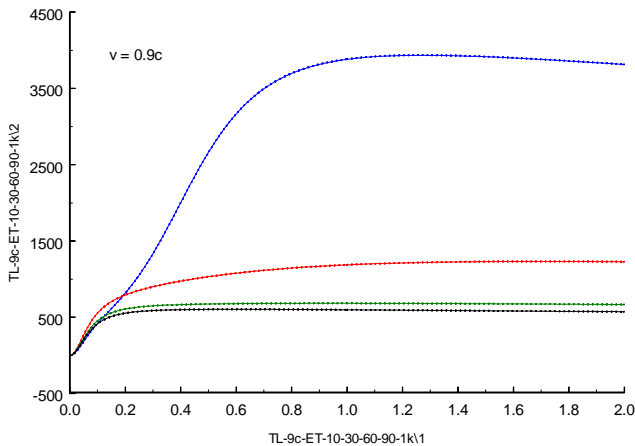


Figure 6b: The θ -component of E-field predicted by the TL model for return stroke speed $v = 0.9c$, above perfectly conducting ground at a distance of 1000 m from channel-base. Other details are as in the caption of Fig. 3b.

5.2 Magnetic fields

Magnetic fields are calculated using equation (10) expressed completely in terms of current and equation (38) expressed completely in terms of apparent charge density. As before the TL model of return stroke is assumed. The effect of a perfectly conducting ground plane is added in all calculations. Figs. 9-15 show the complete agreement between the current formulation (solid line) and apparent charge formulation (dashed line). Magnetic fields at a return stroke speed equal the speed of light (the upper-bound case), and assuming the TL model, can be calculated using an exact simplified

expression given by Thottappillil *et al.* [12, 13] as in [43].

$$\vec{B} = \hat{\phi} \frac{1}{2\pi\epsilon_0 c^2 r \sin \theta} i(0, t - r/c) \quad (43)$$

Equation (43) is equivalent to the sum of equation (10) and similar equation for the image channel. Comparing (41) and (43) it can be seen that ratio of E/B is equal to the speed of light at all angles and distances. Therefore magnetic fields for return stroke speed equal to the speed of light are similar in shape to the electric fields shown in Fig. 8 and also to the channel-base current, provided TL model of return stroke is assumed.

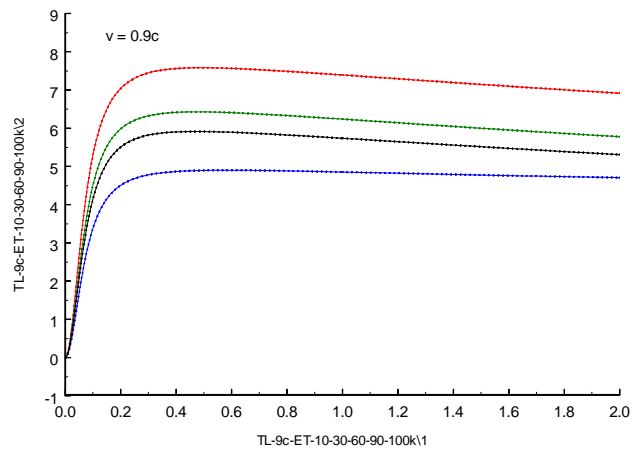


Figure 7: The θ -component of E-field predicted by the TL model for return stroke speed $v = 0.9c$, above perfectly conducting ground at a distance of 100 km from channel-base. Other details are as in the caption of Fig. 4.

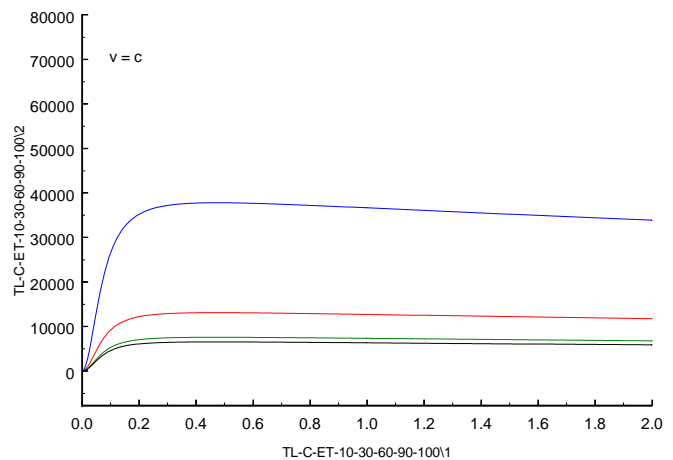


Figure 8a: The θ -component of the E-field predicted by the TL model for return stroke speed $v = c$ (the upper-bound case), above perfectly conducting ground at a distance of 100 m from channel-base. The r-components are identically zero at all angles.

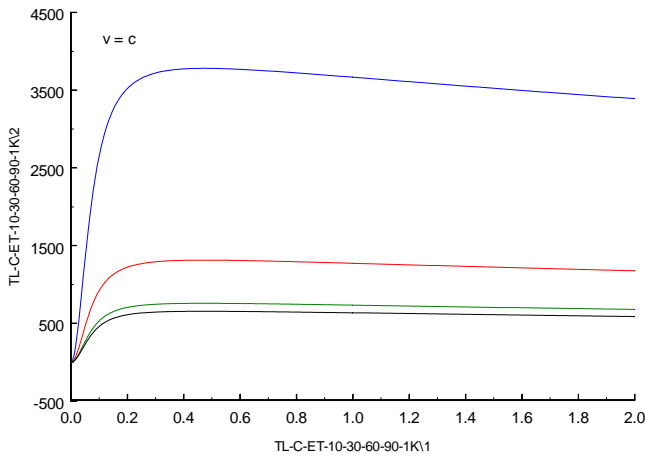


Figure 8b: The θ -component of the E-field predicted by the TL model for return stroke speed $v = c$ (the upper-bound case), above perfectly conducting ground at a distance of 1000 m from channel-base. The r-components are identically zero at all angles.

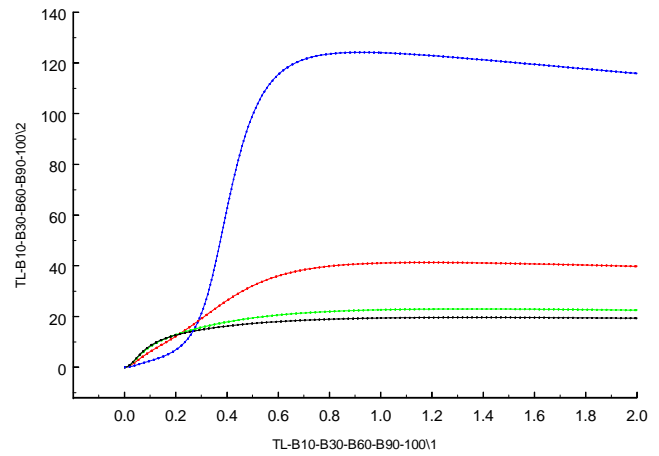


Figure 9: The magnetic field predicted by the TL model for return stroke speed $v = 0.5c$, above perfectly conducting ground at a distance of 100 m from channel-base. Solid line - current formulation, dotted line - apparent charge formulation. The two types of lines (fields for two formulations) are indistinguishable in the plot. Blue - 10° , Red - 30° , Green - 60° , Black - 90° (angle is measured with respect to vertical). Time in μs on the x-axis and E-field in V/m on the y-axis.

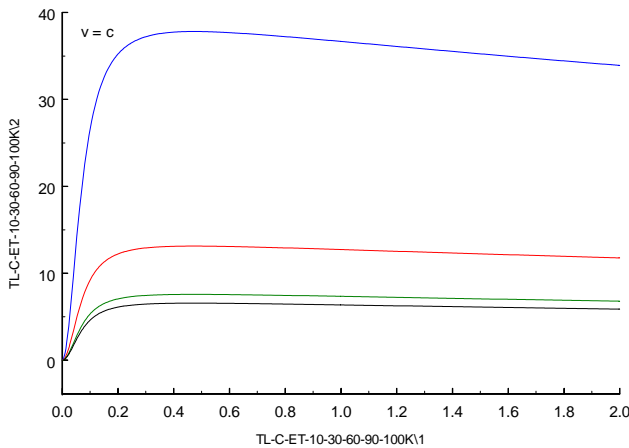


Figure 8c: The θ -component of the E-field predicted by the TL model for return stroke speed $v = c$ (the upper-bound case), above perfectly conducting ground at a distance of 100 km from channel-base. The r-components are identically zero at all angles.

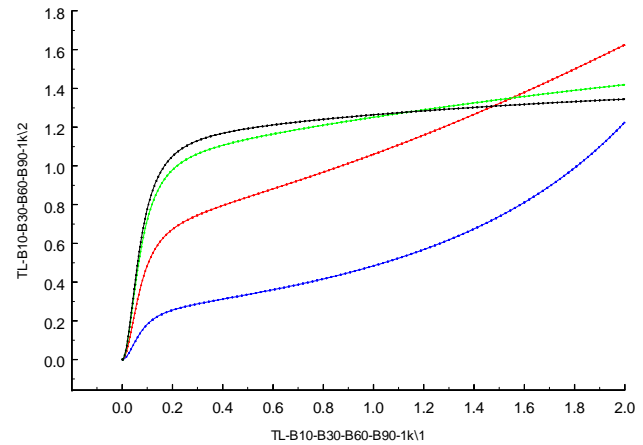


Figure 10: The magnetic field predicted by the TL model for return stroke speed $v = 0.5c$, above perfectly conducting ground at a distance of 1000 m from channel-base. Solid line - current formulation, dotted line - apparent charge formulation. The two types of lines (fields for two formulations) are indistinguishable in the plot. Blue - 10° , Red - 30° , Green - 60° , Black - 90° (angle is measured with respect to vertical). Time in μs on the x-axis and E-field in V/m on the y-axis.

At close distances (100 m and 1000 m) magnetic field has the largest peak value at small angles for all return stroke speeds. However, at a far distance of 100 km, where the field is almost entirely due to radiation, the magnetic field has the largest peak value at 90° at lower speeds ($v=1.5 \times 10^8$ m/s) and the smallest peak value at 90° for the limiting value of speed equal to the speed of light. At a speed of 2.7×10^8 m/s, the maximum radiation is at an angle between 10° and 90° .

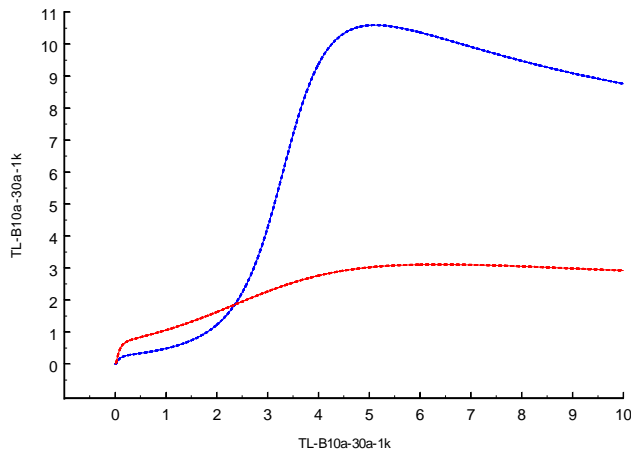


Figure 11: Same as in Fig. 10, but $\theta=10^\circ$ and $\theta=30^\circ$ shown on a time scale of 10 μ s.

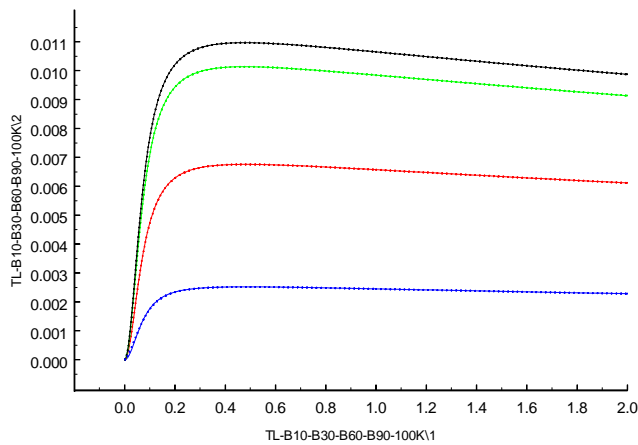


Figure 12: The magnetic field predicted by the TL model for return stroke speed $v = 0.5c$, above perfectly conducting ground at a distance of 100 km from channel-base. Solid line - current formulation, dotted line - apparent charge formulation. The two types of lines (fields for two formulations) are indistinguishable in the plot. Blue - 10° , Red - 30° , Green - 60° , Black - 90° (angle is measured with respect to vertical). Time in μ s on the x-axis and E-field in V/m on the y-axis.

As mentioned earlier, the TL model is used for the numerical calculations for the fields at an elevation presented in Figs 2-15 for the current formulation and the apparent charge formulation. The authors have also compared the numerical calculations for the two formulations using other types of return stroke models, namely, the modified transmission line model with exponential decay (MTLE) as well as linear decay (MTLL), and the Travelling Current Source (TCS) model. Excellent agreement was obtained for the

fields from the two formulations in those cases also. Thus, the equivalence between Equations (9) and (35) is shown both analytically and numerically.

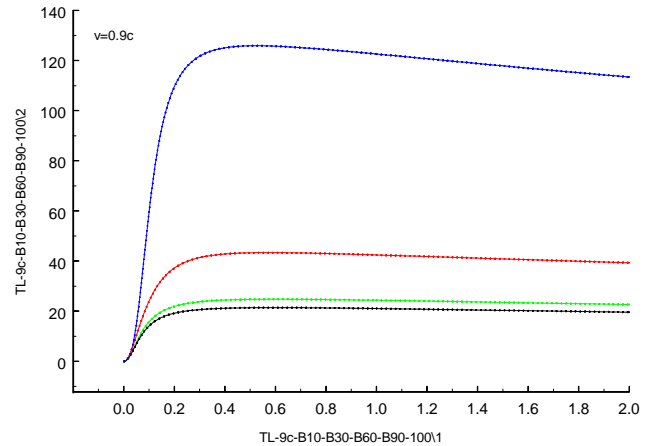


Figure 13: The magnetic field predicted by the TL model for return stroke speed $v = 0.9c$, above perfectly conducting ground at a distance of 100 m from channel-base. Other details are as in the caption of Fig. 9.

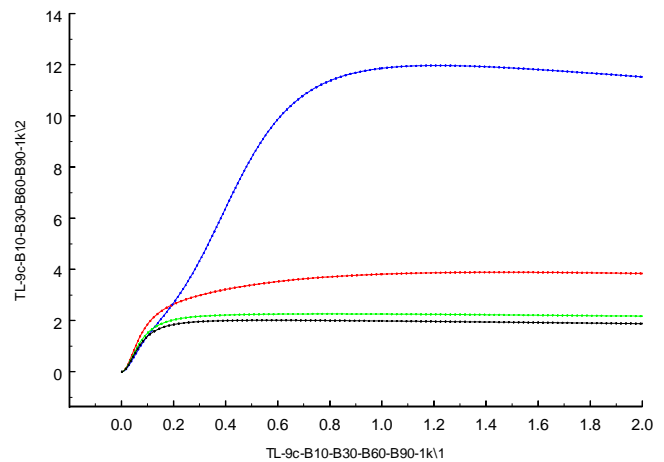


Figure 14: The magnetic field predicted by the TL model for return stroke speed $v = 0.9c$, above perfectly conducting ground at a distance of 1000 m from channel-base. Other details are as in the caption of Fig. 10.

6 CONCLUSION

In this paper three different approaches to the computation of lightning electromagnetic fields are reviewed and their equivalence established. These approaches are the traditional dipole (Lorentz condition) technique, the monopole (continuity

equation) technique and the apparent charge density technique. The latter two techniques are based on two different formulations of the continuity equation, the difference between the formulations being related to different treatments of retardation effects. It is shown that the individual electric field components in the time domain, traditionally identified by their distance dependence as electrostatic, induction, and radiation terms, are different in two of the approaches, suggesting that explicit distance dependence is not an adequate identifier. It is shown that the so identified individual field components in the electric field equation in terms of charge density derived by *Thottappillil et al.* [5] are equivalent to the corresponding field components in the traditional equation for electric field in terms of current based on the dipole technique. However, the individual field components in the electric field equation based on the monopole approach are not equivalent to their counterparts in the traditional dipole technique equation. Further, in the apparent charge density technique and in the traditional dipole technique, the gradient of scalar potential contributes to all three electric field components, while in the monopole technique it contributes only to the electrostatic and induction components. Calculations of electric fields at different distances from the lightning channel show that the differences between the corresponding field components identified by their distance dependence in different techniques are considerable at close ranges but become negligible at far ranges.

If the return-stroke is modeled as a pulse propagating from a source at the bottom of the channel without attenuation and distortion (TL model), then the component of the electric field in the \hat{r} -direction (in spherical coordinate with origin at channel base) reduces in amplitude as the return stroke speed is increased and identically vanishes at return stroke speed equal speed of light (the upper-bound of speed). In that particular case the fields form a TEM field structure with the Poynting vector radially directed away from the source at channel base, and the wave impedance given everywhere by free space impedance [13].

At close distances (100 m and 1000 m) both the electric field and the magnetic field has the largest peak value at small angles from the vertical for all return stroke speeds. However, at a far distance of 100 km, where the field is almost entirely due to radiation, the field has the largest peak value at 90° at lower speeds ($v=1.5 \times 10^8$ m/s) and the smallest peak value at 90° for the limiting value of speed equal to the speed of light. However, whatever be the angle the far fields are always the largest for return stroke speed equals light speed, but the same is not true for fields at very close distances. Above a critical speed less than the speed of light, the largest peak value for the field occurs at an angle less than 90° .

At closer distances (100 m and 1000 m), the peak electric fields decreases with increasing return stroke speed whereas at far distance there is an opposite trend in which the far fields increase dramatically with increasing speed. The linear dependence of the far field peak on the speed of the return stroke is valid only for $\theta=90^\circ$. At other angles, the dependence of the far field peak on the speed is complicated and much stronger than the linear dependence would suggest.

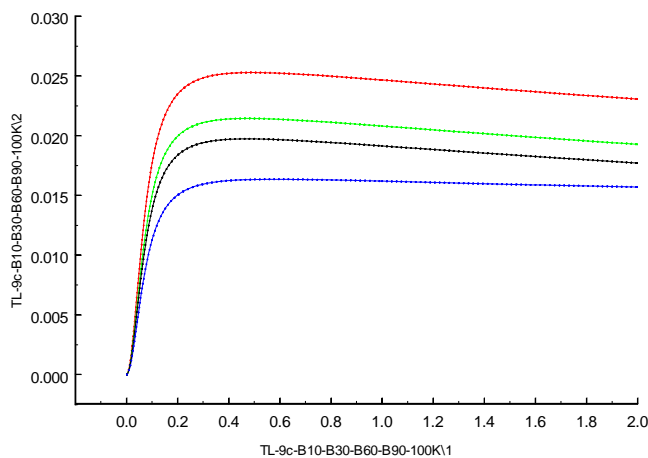


Figure 15: The magnetic field predicted by the TL model for return stroke speed $v = 0.9c$, above perfectly conducting ground at a distance of 100 m from channel-base. Other details are as in the caption of Fig. 12.

7 APPENDIX

The continuity equation and the relationship between charge density and current in the lightning return stroke channel

Continuity equation expresses the principle of charge conservation and is a fundamental law. *Thottappillil and Rakov* [3] has investigated this with an example of a linear element having only one spatial dimension.

Consider a current-carrying channel segment of length $\Delta z'$ whose center (midpoint) M is at a height z' (Fig. A1). Let $q^*(z', t^*)$ be the charge contained in the segment at time t^* . Associated with $q^*(z', t^*)$ is a line charge density which is defined as

$$\rho^*(z', t^*) = \lim_{\Delta z' \rightarrow 0} \frac{q^*(z', t^*)}{\Delta z'} \quad (A1)$$

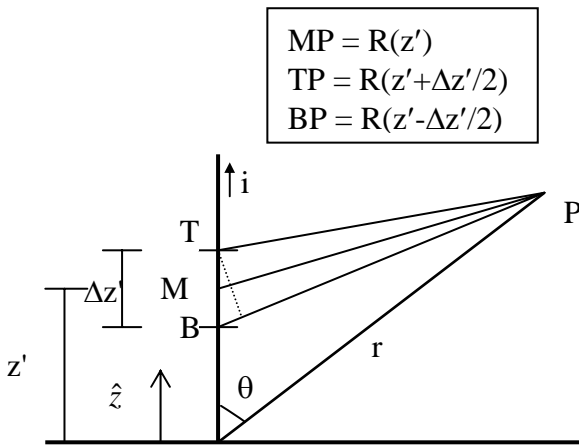


Figure A1: Geometry for explaining the physical meaning of two formulations of the continuity equation, which differ in how retardation effects are accounted for (Adapted from Thottappillil and Rakov [2001a]).

Charge conservation principle requires that a positive rate of change of charge in segment $\Delta z'$ is equal to a negative net outflow of current from the segment. That is,

$$\frac{\partial q^*(z', t^*)}{\partial t^*} = - \left(i(z' + \frac{\Delta z'}{2}, t^*) - i(z' - \frac{\Delta z'}{2}, t^*) \right) \quad (A2)$$

Note that currents at the top and bottom boundaries (T and B) of the segment are specified at the same local time t^* . Dividing through by $\Delta z'$ and letting $\Delta z' \rightarrow 0$ we can obtain the continuity equation

$$\frac{\partial \rho^*(z', t^*)}{\partial t^*} = - \frac{\partial i(z', t^*)}{\partial z'} \quad (A3)$$

with t^* kept constant while carrying out the partial differentiation with respect to z' . The local time t^* could as well be $t - R(z')/c$, where t is the time measured at a remote observation point P at a distance $R(z')$ from the midpoint of the segment, as shown in Fig. A1. Then we can write the continuity equation as

$$\frac{\partial \rho^*(z', t - R(z')/c)}{\partial t} = - \frac{\partial i(z', t - R(z')/c)}{\partial z'} \Bigg|_{t - \frac{R(z')}{c} = \text{const.}} \quad (A4)$$

Note that keeping the time $t - R(z')/c$ a constant in equation (A4) implies that the current crossing the boundary of the element $\Delta z'$ is measured simultaneously at time $t - R(z')/c$. If the currents crossing the ends T and B send a signal to the observer at a certain time then these signals arrive at a remote point simultaneously only if the remote point is equidistant from the ends T and B. An observer on a line passing through the mid-point M of the segment and perpendicular to the segment can receive the signals from the end points simultaneously. Any observer away from this line, such as P in Fig. A1 can not receive the signal simultaneously from the end points because of different travel times for the signals. Now let us see the relationship between the charge and current in segment $\Delta z'$ as viewed from point P.

An observer at P does not “see” the currents at the top (T) and bottom (B) of the segment at the same time. The current at T that observer ‘sees’ at a given time t is from an earlier time $t - R(z' + \Delta z'/2)/c$ and the current at B is from a different earlier time $t - R(z' - \Delta z'/2)/c$. If the difference in the current from the endpoints is interpreted as the rate of change of charge in the segment, then the rate of change of charge in the channel segment as ‘seen’ by the observer at P is

$$\frac{\partial q(z', t - R(z')/c)}{\partial t} = - \left(i(z' + \frac{\Delta z'}{2}, t - R(z' + \frac{\Delta z'}{2})) - i(z' - \frac{\Delta z'}{2}, t - R(z' - \frac{\Delta z'}{2})) \right) \quad (A5)$$

Dividing through by $\Delta z'$ and letting $\Delta z' \rightarrow 0$, we can get equation

$$\frac{\partial \rho(z', t - R(z')/c)}{\partial t} = - \frac{\partial i(z', t - R(z')/c)}{\partial z'} \quad (A6)$$

that relate charge density and current in the channel as ‘seen’ by observer at P.

The line charge densities in equation (A4), ρ^* , and in equation (A6), ρ , are different. In equation (A6), the partial differentiation of retarded current with respect to the source co-ordinate z' is carried out without keeping the retarded time constant; that is, the ‘total’ partial derivative of retarded current is taken. Equation (A4) gives the local charge density or ‘real charge density’ at retarded time, while equation (A6) gives the ‘apparent charge density’ or charge density as ‘seen’ by the

remote observer. Both charge densities can be used in calculating electric fields.

We can now find a relationship between the two charge densities ρ^* and ρ , corresponding to equations (A4) and (A6), respectively. The total partial derivative of retarded current with respect to z' can be written as

$$\frac{\partial i(z', t - R(z')/c)}{\partial z'} = \frac{\partial i(z', t - R(z')/c)}{\partial z'} \Big|_{t - \frac{R(z')}{c} = \text{const.}} + \frac{\partial i(z', t - R(z')/c)}{\partial(t - R(z')/c)} \frac{\partial(t - R(z')/c)}{\partial z'} \quad (A7)$$

We know that

$$R(z') = \sqrt{r^2 + z'^2 - 2rz' \cos \theta}, \quad (A8a)$$

and

$$\frac{\partial R(z')}{\partial z'} = \frac{z' - r \cos \theta}{R(z')}. \quad (A8b)$$

Therefore

$$\frac{\partial(t - R(z')/c)}{\partial z'} = - \frac{z' - r \cos \theta}{cR(z')} \quad (A9)$$

and

$$\frac{\partial i(z', t - R(z')/c)}{\partial(t - R(z')/c)} = \frac{\partial i(z', t - R(z')/c)}{\partial t} \quad (A10)$$

Substituting equations (A9) and (A10) in equation (A7) and rearranging the terms we obtain,

$$\frac{\partial i(z', t - R(z')/c)}{\partial z'} \Big|_{t - R/c = \text{const.}} = \frac{\partial i(z', t - R(z')/c)}{\partial z'} + \frac{z' - r \cos \theta}{cR(z')} \frac{\partial i(z', t - R(z')/c)}{\partial t} \quad (A11)$$

Applying (A4) and (A6) to (A11), we get the relationship between the two charge densities as

$$\frac{\partial \rho(z', t - R(z')/c)}{\partial t} = \frac{\partial \rho^*(z', t - R(z')/c)}{\partial t} + \frac{z' - r \cos \theta}{cR(z')} \frac{\partial i(z', t - R(z')/c)}{\partial t} \quad (A12)$$

where the second term on the right-hand side can be viewed as an adjustment term for the time rate of change of local charge density. Integration of both sides of equation (A12) over time yields

$$\rho(z', t - \frac{R(z')}{c}) = \rho^*(z', t - \frac{R(z')}{c}) + \frac{z' - r \cos \theta}{cR(z')} i(z', t - \frac{R(z')}{c}) \quad (A13)$$

The factor $\frac{z' - r \cos \theta}{cR(z')} = - \frac{\partial(R/c)}{\partial z'}$ is the negative rate of change of time retardation with respect to z' .

In short, equations (A4) and (A6) are two forms of the continuity equation, the former can be viewed as the local continuity equation in retarded time relating real charges and current on the channel and the later can be viewed as the retarded form of the continuity equation in retarded time relating apparent charges (or charges as seen by observer) and the current.

8 ACKNOWLEDGEMENT

The first author acknowledges the support from the donation fund of B. John F. and Svea Andersson and the Swedish Research Council Grant (VR Grant 621-2005-5939). The second author received support from the US National Science Foundation.

9 REFERENCES

- [1] Rubinstein, M., and M.A. Uman, "Methods for calculating the electromagnetic fields from a known source distribution: Application to lightning," *IEEE Trans. Electromagn. Comp.*, 31, 183-189, 1989.
- [2] Safaeinili, A., and M. Mina, "On the analytical equivalence of electromagnetic fields solutions from a known source distribution," *IEEE Trans. Electromagn. Compat.*, 33, 69-71, 1991.
- [3] Thottappillil, R., V.A. Rakov, "On different approaches to calculating lightning electric fields, *Journal of Geophysical Research*," 106, 14191-14205, 2001a.
- [4] Thottappillil, R., and V.A. Rakov, "On the computation of electric fields from a lightning discharge in time domain," 2001 IEEE EMC International Symposium, Montreal, Canada, Aug. 13-17, 2001b.
- [5] Thottappillil, R., V.A. Rakov, and M.A. Uman, "Distribution of charge along the lightning channel: Relation to remote electric and magnetic fields and to return-stroke models," *J. Geophys. Res.*, 102, 6987-7006, 1997.

- [6] Uman, M. A., D. K. McLain, and E. P. Krider, "The electromagnetic radiation from a finite antenna," *Am. J. Phys.*, 43, 33-38, 1975.
- [7] Jefimenko, O.D., *Electricity and magnetism*, Second edition, Electret Scientific Company, Star City, USA, 1989.
- [8] Thomson, E.M., "Exact expressions for electric and magnetic fields from a propagating lightning channel with arbitrary orientation," *J. Geophys. Res.*, 104, 22293-22300, 1999.
- [9] Rubinstein, M. and M. A. Uman, "On the radiation field turn-on term associated with travelling current discontinuities in lightning," *J. Geophys. Res.*, 95, 3711-3713, 1990.
- [10] Thottappillil, R., M. A. Uman, and V. A. Rakov, "Treatment of retardation effects in calculating the radiated electromagnetic fields from the lightning discharge," *J. Geophys. Res.*, 103, 9003-9013, 1998.
- [11] Rakov, V.A., and M.A. Uman, "Lightning: Physics and Effects," Cambridge University Press, Cambridge, UK, 2003.
- [12] Thottappillil, R., J. Schoene, and M.A. Uman, "Return stroke transmission line model for stroke speed near and equal that of light," *Geophysical Research Letters*, 28, 3593-3596, 2001.
- [13] Thottappillil, R., M.A. Uman, N. Theethayi, "Electric and magnetic fields from a semi-infinite antenna above a conducting plane," *J. Electrostatics*, 61, 209-221, 2004.
- [14] Nucci, C.A., Diendorfer, G., Uman, M.A., Rachidi, F., Ianoz, M., and Mazzetti, C., "Lightning return stroke current models with specified channel-base current: a review and comparison," *J. Geophys. Res.* 95: 20,395-408, 1990.
- [15] Krider, E.P., "On the peak electromagnetic fields radiated by lightning return strokes toward the middle-atmosphere," *J. Atmos. Electr.*, 14, 17-24, 1994.
- [16] Rakov, V.A., and W.G. Tuni, "Lightning Electric Field Intensity at High Altitudes: Inferences for Production of Elves," *J. Geophys. Res.*, Vol. 108, No. D20, 4639, doi: 10.1029/2003JD003618, 2003.